*Acta Polytechnica* **59**(1):77–87, 2019
doi:10.14311/AP.2019.59.0077


# EVALUATION OF RAILWAY BALLAST LAYER CONSOLIDATION AFTER MAINTENANCE WORKS

Mykola Sysyn[a,*], Olga Nabochenko[b], Vitalii Kovalchuk[b], Ulf Gerber[a]

[a] *Technical University of Dresden, Hettnerstr. 1/3, Dresden, Germany*
[b] *Dnipropetrovsk National University of Railway Transport, Blagkevich 12a, Lviv, Ukraine*
[*] corresponding author: mykola.sysyn@tu-dresden.de

Abstract. The results of the study of the ballast layer consolidation after the work of ballast-tamping machines of different types are given in the article. The existing methods of determining the degree of consolidation of the ballast layer are analysed. The seismic method was improved by means of a complex dynamic and kinematic interpretation of the impulse response. For the dynamic interpretation with the use of statistical analysis, the features are selected so that they correspond to the degree of consolidation of the ballast layer. On the basis of researches, a device and software were developed that allow an automated evaluation of the ballast layer consolidation based on the kinematic and dynamic analysis of the measured impulse response. The measurements of the degree of the ballast layer consolidation after an operation of ballast-consolidation machines in different sequences allowed establishing the efficiency of the consolidation and the feasibility of the machines' application.

Keywords: ballast layer consolidation; tamping machines; seismic method; impulse response interpretation; signal processing; feature selection; classification; clustering.

## 1. Introduction

The long-term deformation of the track geometry, in great extent, depends on the initial quality of the track. One of the most effective means to improve the track operation is to achieve the highest possible initial quality of the track during its construction [1–6]. At present, the quality of the construction of the ballast layer and its consolidation is estimated by the stability of the track geometry. The degree of the ballast layer consolidation corresponds to its greatest bearing capacity and resistance to a shape change. The information about the degree of the ballast consolidation under sleepers is important because it gives the possibility to evaluate the quality of the repair works, as well as further deformation of the track geometry. As studies show [7–11], a well-consolidated ballast layer after the track repair enables to significantly extend the lifecycle period of the ballasted track and track structures. Among the known non-destructive methods (NDM) of the soil consolidation degree determination are the following: pneumatic, hydrometric, radiometric (isotope), radio engineering, seismic, hammer test and others. The author of the research [12] gives the classification of possible methods of the crushed stone consolidation (Figure 1).

The seismic methods and radio engineering techniques found a wide field of application. The Falling Weight Deflectometer (FWD) is a method for measuring the subgrade elasticity, which is based on the measurement of the velocity response of the soil oscillation under the influence of the impulsed load caused by some falling mass [13]. This method is adapted to measure the ballast layer elasticity of the railways. The Sonic Echo method measures the time of the wave propagation from the impact point through the ballast and back to the sensor. The accelerometer is used as a receiver, as a rule, and the created oscillation excitation is relatively small, usually with a 1 kg of mass. The result of the measurement is the time-shift in oscillation impulses. With a known thickness of the ballast layer, one can draw the conclusion for the ballast consolidation. In the method of Ground Penetrating Radar (GPR) [14, 15], instead of the physical wave of oscillation, short impulses of electromagnetic radiation are generated in the soil that are moving from the transmitting antenna to the receiver. The ballast, which has different dielectric properties in depth, reflects different waves of radiation in different ways. According to the amplitude and time of the measured wave's passage, the distribution profile of the heterogeneity of waves' propagation in the ballast layer is constructed. The GPR method can determine the presence of pollutants in the ballast layer, such as fine and clay constituents. However, this method is not suitable for measurement of the initial degree of consolidation of the pure ballast. The measurement of the ballast layer consolidation distribution on the basis of kinematic interpretation after tamping machines [12] with the seismic technique and the device UVP-DIIT were applied. The method is based on the techniques from seismic survey. The traditional field of seismic survey application is the study of relatively homogeneous masses of soils of a large size. Unlike the soil, the railway track is more complicated object in terms of the design and variety of material prop-

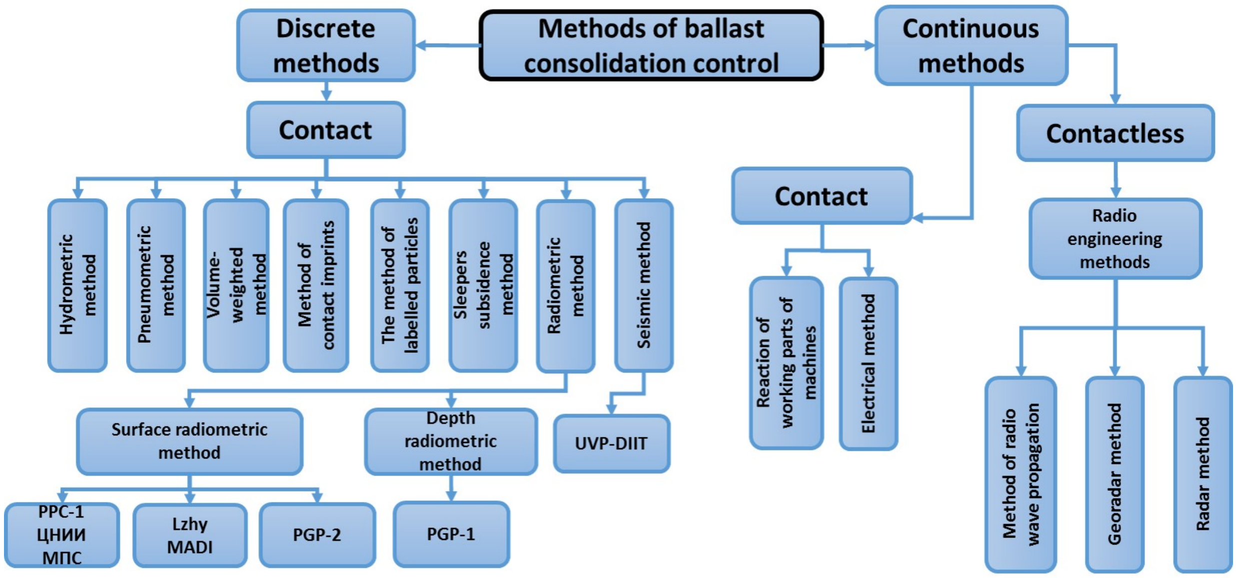


Figure 1. Monitoring methods of ballast layer consolidation [12].

erties. The impact of sleepers and the subgrade can be considerable on the overall measurement result. In most cases, the soil density analysis uses the method of kinematic interpretation of a signal, which is based on determining the propagation speed or time of flight (TOF) of the acoustic impulse in an elastic medium. The method uses only the minimal part of the information, recorded by seismic sensors, and does not take into account the whole process of oscillation and its nature. The application of this kinematic method of interpretation, to determine the properties of the ballast layer, is complicated as the track is a physically non-uniform object and the velocity of the impulse propagation is affected not only by the ballast layer, but by other elements too. That is confirmed by a considerable ambiguity and the spread of measured values. In addition, the purpose of kinematic interpretation in seismic investigation was traditionally not to determine the properties of the elastic medium, but to determine the boundaries between different sections of the medium. Recently, the dynamic interpretation of seismic data is increasingly being used, which, in addition to speed, also takes into account the entire recording of the dynamic response signal to the impulsed load, analogous to the methods used in the seismic investigation [13, 16, 17]. Among these methods, spectral methods of dynamic interpretation are increasingly being applied such as the so-called Rail Road Response Factor (RRRF) used to evaluate the condition of the subgrade by means of waves excited by trains of different types and speeds [18]. In addition, non-destructive seismic methods for assessing the dynamic response of the superstructure of the track are used in the so-called Hammer Test [19–23], which is used to evaluate the dynamic properties of the track and the ballast layer in its composition. The peculiarity of the measurements of the ballast layer consolidation is that the results of measurements, in addition to the degree of consolidation, are influenced by many other factors, such as the ballast layer thickness, the influence of sleepers, etc., which determine the nature of the wave passage and distribution in the ballast layer. All the undetermined factors' influence causes considerable deviations of the measurement results. This fact, together with the big number of measurements, demand the application of the computer based processing and data mining methods. The methods, together with laboratory tests, enable to reduce the influence of unknown factors and select the informative features of the ballast consolidation. The data mining methods are widely used in the transportation research. The general methodology of a big data analytics application for a track maintenance planning system is described in the study [24]. The practical application of the methods for the track maintenance is shown in another paper [25] at an example of a track quality index analysis. The data-driven rail-infrastructure monitoring that is based on data fusion, feature extraction, selection and other data mining methods is presented in the literature [26–28]. In the present paper, one part of the data mining is used: the feature extraction and selection, that is based on the statistical classification and clustering methods. The purpose of this experimental study is to establish the effectiveness of ballast tamping with tamping machines and dynamic stabilizers of various designs and an optimal mode of their operation. The problem is solved in 3 subsequent steps:

- development of measurement device together with signal processing software;
- laboratory measurements and consolidation feature selection with statistical learning methods;
- in-situ measurement of ballast consolidation after tamping works.

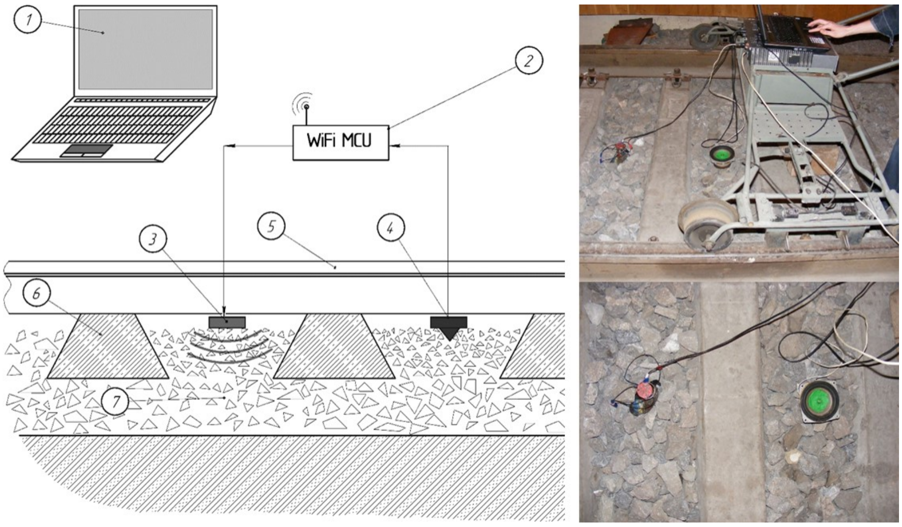


Figure 2. Principal scheme of the device for assessing ballast consolidation: 1 – server for signal processing; 2 – Wi-Fi microcontroller unit with ADC; 3 – electrodynamic emitter of pulse acoustic signal shaker –; 4 – seismic sensor SV-20P; 5 – rail; 6 – sleeper; 7 – ballast layer.

## 2. Experimental measurements of impulse response of the ballast layer with different consolidation degree

The propagation of elastic waves through a grainy medium, which is the ballast layer of the railroad, is determined by the mineralogical and granulometric composition of the grains. To a large extent, it depends on the number of contacts between the grains, that is, the ballast layer consolidation. Thus, by measuring the velocity of the elastic waves propagation after each passage of a dynamic rail stabilizer, it is possible to evaluate the degree of the ballast consolidation. For measurements, a seismic sensor of the type SV-20P is used, which operates on the principle of measuring the velocity of oscillations and the effect of electromagnetic induction [16]. The creation of the impulse in the ballast layer is carried out by means of the plate, which distributes the load between ballast grains on the surface of the ballast layer, and the hammer connected to it in an electric circuit. The source of elastic waves is an impact on the metal disk (diameter 100 mm, height 10 mm), which is placed on the ballast. The size of the plate is enough to provide the simultaneous support on 3 neighboured stones with a maximal size of 60 mm. At the same time, a bigger plate could provide some ambiguity in the interpretation due to a short distance between the receiver and emitter. The registration of the wave velocity was carried out by the digital analyser of UVI-2 type. The emitter is located in the adjacent ballast boxes to the signal receiver along the track axis. In addition, other layout schemes are considered, such as the transverse direction; location through several ballast boxes, etc. The considerations to the optimal measurement scheme are described in the study [29]. The distance between the shaker and the receiver is 0.5–1.5 m. It has been established that the granular medium can be considered as homogeneous with corresponding characteristics at the distance between the shaker and the receiver of approximately $10\,d$ (where $d$ is a mean grain diameter). In parallel with the measurements of the wave passage velocity, the signal recording from the seismic receiver and further kinematic and dynamic analyses based on the developed automatic system were used (Figure 2). The prototype of the device includes the following units:

- electrodynamic emitter of impulsed acoustic signal, which amplitude-frequency characteristic allows to generate signals of the spectrum of low frequencies (shaker);
- amplifier of generated impulsed acoustic signal necessary for amplifying the output signal of the emitter;
- seismic sensor SV-20P;
- MCU (ESP32 programmable microcontroller), which executes, together with a shaker, the command of the server program of the impulse excitation for the numerical registration of the analog signal from the geophone by the module ADS1256 with the frequency of 15 kHz, and sending information to the server for further processing;
- special software that manages the controller, acceptance and processing of the dynamic response signal.

To ensure the operation of the system, the software for the microcontroller was developed, based on the IDE Eclipse. To determine the criteria for evaluating the impulsed ballast feedback, the software was developed using the MATLAB program package [30], which allows plotting the recorded signal with its zooming and viewing functions. The connection with the controller is executed by the wireless protocol UDP. The

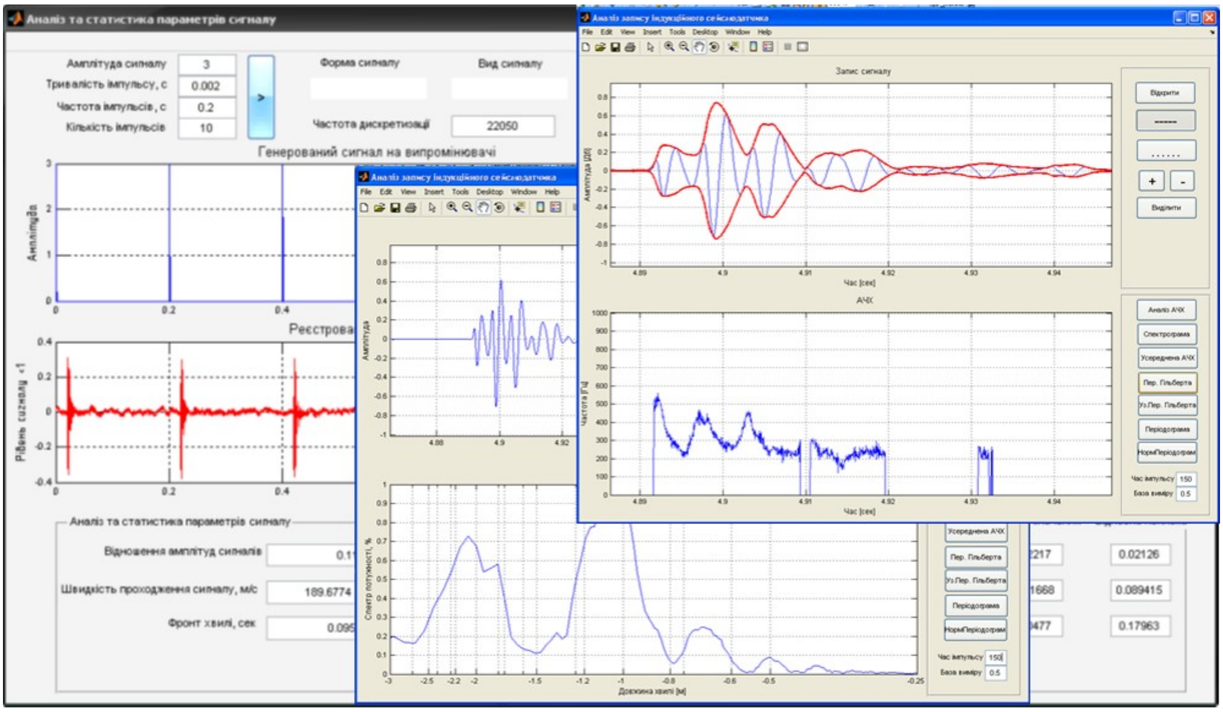


Figure 3. The program interface for measuring and processing the results.

developed software also performs kinematic and dynamic analyses of a signal, or its separate components, using DFT methods or a periodogram with averaging results, and calculates the analytical signal and instantaneous frequency. In addition, the statistical processing of the obtained results is carried out and the need for additional measurements is determined. The processing program example is shown in Figure 3.

## 2.1. Dynamic interpretation and signal processing

The measured response signal is usually quite complex, so there are many ways of interpreting this signal. The most common way is to interpret the frequency response (hereinafter - FR) of the measured signal. Conventionally, a Fourier series is used for this purpose, which allows decomposing the time series of the signal into elementary harmonic components of different amplitudes, frequencies and phases. The disadvantage of this method is that during the Fourier series transformation, a part of the information associated with the time is lost. To eliminate this disadvantage, other criteria for signal evaluating are used: the instantaneous frequency (IF) and the analytical signal found by Hilbert transformation (hereinafter - HT), spectrogram and wavelet analysis [31]. In contrast to the FR, the instantaneous frequency allows detecting the change in the average frequency of oscillations of the response signal during the oscillation time. The analytical signal is a two-way envelope of a real signal and allows it to be simplified in a more perceptible form for an interpretation. The spectrogram and wavelet analyses provide additional interpretation parameters, but also demand the following more complicated statistical processing. Therefore, in this study, it is proposed to analyse the recorded dynamic response of the signal using the two given spectral methods of dynamic interpretation FR and HT, and also to compare the results with the results of the kinematic interpretation, carried out in parallel. A nonparametric periodogram [31] is used in practical calculations of the power spectrum of the discrete signal. The method allows estimating the spectral power and is obtained by N samples of one realization of the random process. The periodogram is calculated by the formula:

$$W(\omega) = \frac{1}{N f_d} \left| \sum_{k=0}^{N-1} x(k) e^{-j\omega k T} \right|^2, \qquad (1)$$

where $T$ – sampling period; $\omega k$ – signal spectrum; $f_d$ – sampling rate; $x(k)$ – signal data.

In addition to the criterion of the signal spectrum, the criteria of the analytical signal and instantaneous frequency are used to estimate the ballast layer consolidation. In the frequency analysis of the dynamic ballast response with the help of the discrete Fourier transform (DFT), the important information is obtained about the spectral composition of the signal, however, the part of the information that corresponds to the time of each component during the oscillation period is lost. As it is known from experimental and theoretical studies, the waves of different frequencies occupy different areas in the elastic environment and pass different paths from the emitter to the receiver. Therefore, one should expect that high spectra should dominate at the beginning of the signal at these measurements. However, the peculiarity of the dynamic response in elastic environments is that the dynamic response, recorded by the receiver, always has a stable harmonic component regardless of the shape and duration of the load pulse of the emitter. Thus, the task of evaluating the dependence of the oscillation parameters on time is raised. Taking into account the existing problem as well as the properties of the signal, you can replace the actual signal $S(t)$ with a combination of three functions:

$$S(t) = A(t) \cdot \cos(\omega_0 \cdot t + \phi(t)), \tag{2}$$

where $A(t)$, $\phi(t)$ – amplitude and phase, which are functions of time. In the complex, form $S(t)$ can be represented by the real part of the analytic signal $z(t)$:

$$z(t) = S(t) + S_\perp(t), \tag{3}$$

where $S_\perp(t)$ – conjugate signal. In exponential form, the dependence (2) has the form:

$$z(t) = A(t) \cdot e^{i\phi(t)}, \tag{4}$$

where $\Phi(t)$ – instantaneous phase.

The unknown component is a conjugate signal $S_\perp(t)$. To find it, Hilbert's conversion is used:

$$S_\perp(t) = \frac{1}{\pi} \int_{-\infty}^{\infty} \frac{S(t')}{t - t'} \, \mathrm{d}t'. \tag{5}$$

The conjugate signal found in this way is used to determine the instantaneous values of the amplitude $A(t)$, phase $\phi(t)$ and frequency $\omega(t)$:

$$\begin{aligned} A(t) &= \sqrt{S^2(t) + S_\perp^2(t)}, \\ \phi(t) &= \operatorname{arctg} \frac{S_\perp(t)}{S(t)}, \\ \omega(t) &= \frac{\mathrm{d}\phi(t)}{\mathrm{d}t} = \frac{S'_\perp(t) \cdot S(t) - S'(t) \cdot S_\perp(t)}{S^2(t) + S_\perp^2(t)}. \end{aligned} \tag{6}$$

The function $A(t)$ is a two-way enveloping signal $S(t)$ and is also called an analytic signal. The instantaneous frequency $\omega(t)$ differs from the frequency of spectral components by the fact that, at a certain point of time, it takes only one value and the number of components with different frequencies for one instant of time may be infinite. Unlike the DFT, this technique rejects the part relating to the distribution of the signal by spectra. Before the field measurements, to determine the characteristic features, the laboratory bench test measurements were performed. After that, field measurements were made on the sections of the track where repairs were carried out. For comparative values of the criteria acquisition, the measurements were initially carried out during the laboratory bench tests on consolidated and unconsolidated crushed stone, and then the natural measurements on the track were carried out. The most rational arrangement of the signal emitter and receiver on the track was chosen.

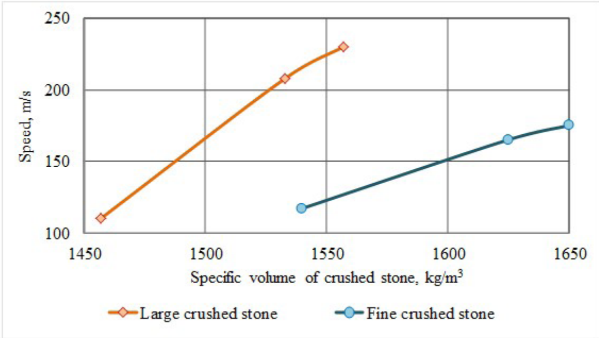


Figure 4. The dependence of wave propagation velocity on consolidation of the crushed stone layer.

## 2.2. Laboratory tests

To determine the characteristic features of the difference between consolidated and unconsolidated ballast, the laboratory research was carried out on a special test-bench that allows creating consolidated ballast. The box of $1.05 \times 0.70 \times 0.80$ m size, filled with crushed stone, was used as a test-bench. This box was filled with railroad crushed stone mixture of 0.60 m depth without consolidation. The degree of its compaction is calculated as the ratio of the mass of crushed stone to its volume. This is the least consolidated ballast. The three levels of compaction are considered: maximum unconsolidated, maximum consolidated and intermediate. Then a gradual consolidation of the ballast is performed with the help of a vibro-plate, which is attached to the electric track-tamping machine. At the same time, at each stage of the compaction, the measurements of the wave passage velocity from the striker to the receiver are carried out. The measurements and records are performed on the basis of 0.5 m according to the described algorithm. Different conditions of contact of the sensor with the ballast are considered. According to measured data, a kinematic and dynamic interpretation of the impulse response is performed. The results of the kinematic interpretation can be seen in the form of graphs of dependence of the wave propagation velocity on the density of crushed stone (Figure 4). As it can be seen from the diagram, the fine crushed stone is consolidated more than the railroad crushed stone mixture, and the amount of fine crushed stone reaches 1650 kg/m$^3$ in comparison with 1550 kg/m$^3$ of the railroad crushed stone mixture. Comparing the data obtained during the research, we can make conclusions about the crushed stone consolidation in the experimental sections of the railway.

## 2.3. Selection of informative features for consolidation

For a statistically substantiated determination of characteristic features of the ballast consolidation or unconsolidated, a special statistical analysis is carried out. It consists of the complex analysis and identification of common and distinctive features of the periodograms

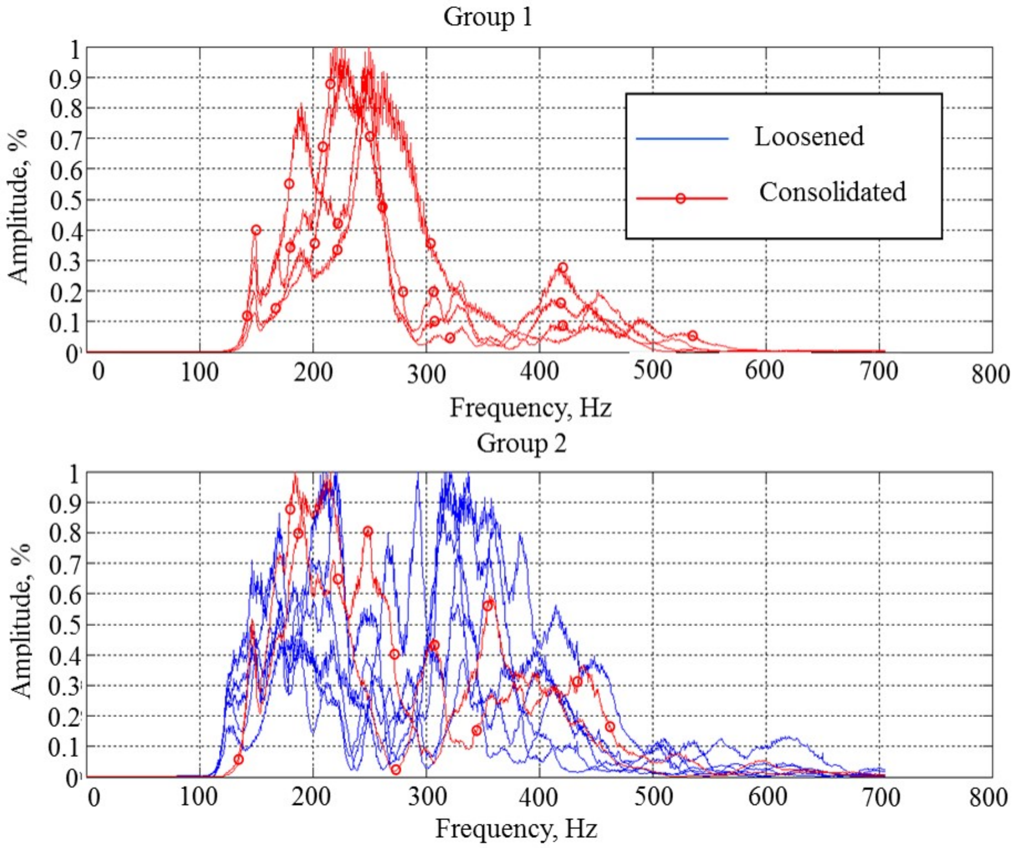


Figure 5. The results of distribution into two hierarchical clusters without taking into account measurement amplitude.

by the cluster and classification analysis [32]. The cluster analysis can give the answer, which groups the aggregated multivariate experimental data collected in the general sample can be divided into, but it does not show according to which characteristic features one or another group can be distinguished. In this study, the hierarchical cluster grouping method is used. The above mentioned methods of classification and grouping are used initially for the analysis of laboratory measurements. The group of laboratory measurements includes 12 records of the impulse response of the consolidated and unconsolidated crushed stone under different contact conditions. Since, in this study, the amplitude of the signal is a rather subjective value, which depends on the contact of the excitation source, the crushed stone and the sensor, this value is neglected, and the amplitude result is shown in a percentage of the maximum value. In the cluster hierarchical analysis, measurements are divided into groups using the similarity measure to the type of the correlation. The results of distribution among two groups without taking into account the amplitude of measurements are shown in Figure 5. Each of the charts showing the two most distinct groups. The group in the Figure 5a contains only the periodograms of measurements of the consolidated ballast. The group in Figure 5b contains two periodograms of measurements of the consolidated ballast and all periodograms of measurements of the unconsolidated ballast.

While considering the entire range of periodograms in the graphs, it is impossible to answer definitely, whether the ballast is consolidated or not. However, if we consider only the initial frequency range 0 to 200 Hz, the division into clusters is carried out without errors. Figure 6 shows the clusters in the frequency range 60–150Hz for a better visualization.

This distinctive signal recognition is due to the fact that there is a significant difference between the periodograms of the signals in consolidated and unconsolidated ballast in this range of the spectrum. The inaccurate grouping of periodograms of signals while considering the entire spectrum of the signal is due to the fact that the expressed similarity at the beginning of the section is mixed in the general statistical uncertainty of the rest of the spectrum. The cluster analysis statistically confirms that the measurements made can be rather accurately attributed to measured groups. Therefore, it can be assumed that there is a certain set of informative features that allow referring periodograms of signals to one or the other group. To find them, the linear discriminant analysis is performed [33]. The results are shown at Figure 7 with 2 double vertical axes that correspond to average power spectral densities for unconsolidated and compacted ballast together with the measure of

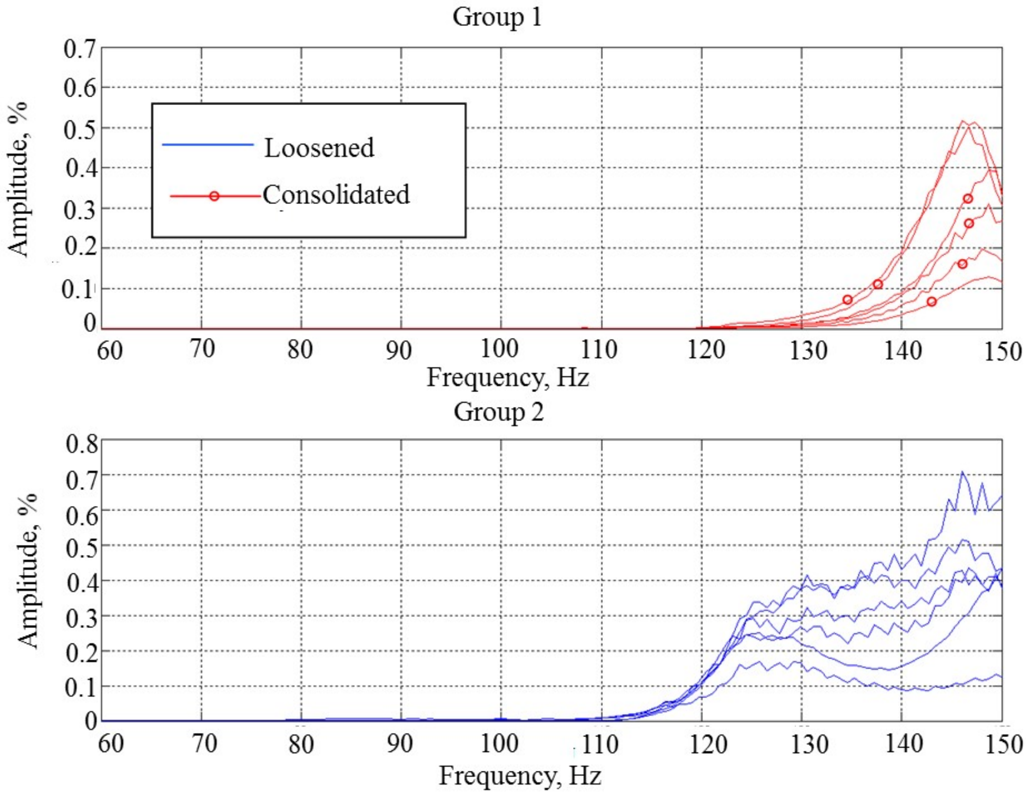


Figure 6. The results of division into two hierarchical clusters while considering part of a signal spectrum 60 to 150 Hz.

the difference. The measure is the Fisher's criterion. Considering Figure 7, one can see that the maximum value of Fisher's criterion $F = 22$ corresponds to the frequency of 118 Hz, with the critical value of Fisher's criterion for 12 levels and probability of 0.95 $Fk = 3.89$ [33]. This means that the value of the frequency near 118 Hz point is representative for evaluating the ballast consolidation. In this case, the estimation of the difference of signals periodograms according to Fisher's criterion is performed over the entire frequency range, which shows that the distinction between the groups of signals is different at various frequencies of the spectrum. Hereinafter, the selected frequency feature will be called the low side spectrum (LSS).

It is possible to conclude that the maximum consolidated ballast state under laboratory conditions corresponds to the frequency of the LSS approximated at 122 Hz, and the unconsolidated ballast corresponds to 103 Hz. The graphs of instantaneous frequency change during the response signal passage before and after the ballast consolidation are shown in Figure 8. Considering the graphs, one can see that, at the beginning of the signal (up to 0.0003 s), the prevailing frequency is 450–650 Hz, and the rest average value of frequency is 300 Hz. Large fluctuations of frequency occur due to the signal imposition of direct and reflected waves. This leads to an uncertainty in the frequency estimation.

The greatest difference between the graphs of instantaneous frequency of the consolidated and unconsolidated ballast is observed at the beginning of the oscillation, so this point can be used as a characteristic sign of consolidation. From the physical point of view, the maximum value of the instantaneous frequency is connected with the leading edge of a wave, which corresponds to the time from the beginning of oscillations to the amplitude in the first half-wave of the oscillation and is of an inversely proportional magnitude. The leading edge of a wave is traditionally used in the analysis of physical properties of soils. One of the disadvantages of the leading edge of a wave evaluation is a rather large uncertainty in the determination of the beginning point of the oscillation, caused by the smoothness of growth from zero signal level, which leads to some error. The instantaneous frequency criterion does not have this disadvantage, since only its maximum value is selected. Laboratory studies showed the following results:

- before consolidation, the leading edge of a wave is 0.9285 ms at a relative error of 14.2 %, and the maximum instantaneous frequency of 538.9 Hz with a relative error of 4.01 %;
- after the consolidation, the leading edge of a wave is 0.869 ms at a relative error of 12.9 %, and the maximum instantaneous frequency of 586.1 Hz with a relative error of ±6.71 %.

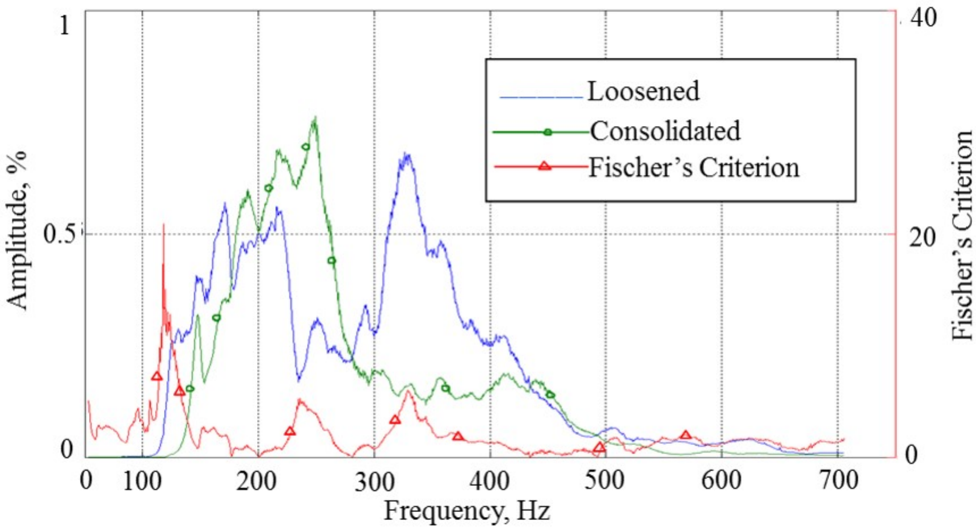


Figure 7. Graphs of averaged values of periodograms of signals for groups of consolidated and unconsolidated ballast and Fisher's criterion value.

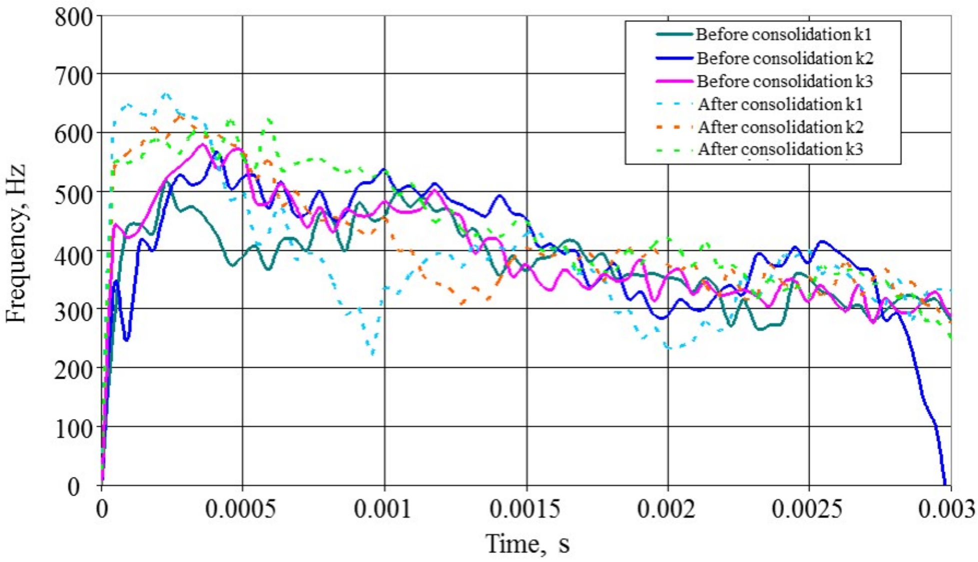


Figure 8. The instantaneous frequency of signals change at the initial signal moment.

The simplified statistical study of the grouping and classification of periodograms of the ballast layer impulse response without a regard to the amplitude obtained under laboratory conditions shows a high degree of reliability of the ballast consolidation assessment and a low error rate.

## 3. In-situ measurements of the ballast layer consolidation after track repair with tamping and stabilization

On the basis of the developed device and the technique, the experimental measurements of the ballast consolidation after the track repair with the use of ballast-tamping machines Duomatic, dynamic stabilizers DGS (produced by Austrian firm Plasser & Theurer) and the DSP (produced by Russian company Remputmash DSP-C4) are performed. The field measurements were performed at the line Khangzhenkovo-Khartsyzsk of Donetska Railway. The 3 km test track was devided into 6 equal parts, 500 m each, with different tamping machine types and number of passages. The absolute settlement measurements were performed with the track levelling immediately after the tamping and after 0.3 and 0.8 Mt. All measurements are made with the base distance of 0.5 m along the axis of the track (the emitter and the receiver are in the neighbouring ballast boxes) at different stages of the ballast consolidation on different sections of the track, where repair works had been carried out. In each case, a group of measurements in 20 neighbouring ballast boxes was made to increase the validity. The reliability of parameter measurements at each ballast box is insured

| No. | Machinery | **LSS** (Hz) | Δ | **WLE** (ms) | Δ | **IF** (Hz) | Δ | **WV** (m/s) | Δ |
|---|---|---|---|---|---|---|---|---|---|
| 1 | HV + DTE | 82.3 | 10.6 % | 0.836 | 8.8 % | 495.7 | 9.2 % | 282 | 36 % |
| 2 | HV + DTE + DGS | 86.5 | 5.9 % | 0.785 | 14.9 % | 526.8 | 13.5 % | 318 | 28 % |
| 3 | HV + DTE + DSP | 96.6 | 4.6 % | 0.659 | 9.7 % | 624.8 | 4.3 % | 336 | 22 % |
| 4 | HV + DTE + 2DSP | 103.6 | 7.9 % | 0.562 | 24.0 % | 641.5 | 11.9 % | 352 | 18 % |

Table 1. The analysis of the results of experimental in-situ measurements: HV – hopper-vagon; DTE – Dynamic Tamping Express (Duomatic 09-3X); DSP – stabilization with DSP (Remputmash); DGS – stabilization with DGS (Plasser & Theurer).

automatically with a repeated number of impacts and measurements until their mean deviation reaches the acceptable value. The errors of measurement are minimized with outlier removal and statistical processing.

The results of the analysis of low side spectrum (LSS), the velocity of wave propagation (WV), the leading edge of a wave (WLE) and the instantaneous frequency (IF), as well as their relative error are given in Table 1.

## 4. Discussion

As it can be seen from the table, the statistical spread of the values of the spectrum beginning, the instantaneous frequency and the leading edge of a wave is much less than the spread of an average velocity of the waves propagation. The results of measurements along the track are taken into account, where the emitter and the receiver are arranged in the neighbouring ballast boxes. The mean value analysis of the LSS showed the following. The LSS increases with the number of the stabilizer passages: 22.9 % and 31.8 % during the second and third passages of the DSP, respectively. That is, the difference of the values of the LSS between the first and second passages was significant and amounted to 22.9 %, while the difference of the values between the second and third passages was negligible and amounted to 8.9 %. After the first passage, the DGS stabilizer showed better results of the LSS compared to DSP: by 4.7 % more at the last composition of the HV in the machine chain and by 10 % more at the last composition of the DTE in the chain. The analysis of the mean values of the leading edge of a wave showed that, with a larger number of passages of the DSP, the leading edge of a wave decreases. Compared to the first and third passages of the DSP, the difference was 39.7 %, and 17.3 % between the second and third passages, respectively. The value of the leading edge of a wave after the first passage of the DGS stabilizer with the subsequent passage of DTE and HV is the largest that corresponds to an unconsolidated crushed stone. The analysis of average values of instantaneous frequency showed the following. The IF increases with the number of stabilizer passages: by 18.6 % and 21.8 % at the second and third DSP passages respectively. That is, the difference of values of the instantaneous frequencies between the first and second passages was significant and amounted to 18.6 %, while the difference of values between the second and third passages was negligible and amounted to 3.2 %. The value of the instantaneous frequency after the first passage of the DGS stabilizer with the subsequent passage of DTE and HV is the smallest, which also corresponds to the unconsolidated crushed stone. Thus, it can be concluded that the first and second passages of the stabilizer are the most effective, and the third passage is unproductive.

## 5. Conclusions

The performed theoretical and laboratory studies have shown that the considered parameters of the impulse response in the ballast have a stable correlation with the degree of the consolidation of the ballast layer. Experimental studies of the degree of the ballast layer compaction after the ballast-consolidating machine's work make it possible to conclude that there is a significant increase in the degree of the consolidation after first passages of ballast-compaction machines. Further passages, while discharging the entire ballast layer, are ineffective. This indicates the necessity of a step-by-step ballast layer discharge and stabilization. As for further research in the field of the determination of the ballast layer consolidation degree, the following directions are promising:

- the study of the interconnection of measured kinematic and dynamic values that characterize the degree of the ballast consolidation with long-term processes of a uniform and uneven subsidence of the ballast layer;
- the forecast for track geometry deformation on the basis of measurements of consolidation degree. The improvement of the seismic technique for the consolidation degree measurement is possible in the following directions:
- multisensory synchronized impulse response measurements;
- measurements of longitudinal and transverse components of oscillation waves based on triaxial accelerometers;
- determination of the spatial distribution of crushed stone consolidation along the sleeper and along the track on the basis of seismotomographic methods.

## List of symbols

**LSS** low side spectrum [Hz]
**WLE** leading edge of a wave [ms]
**IF** instantaneous frequency [Hz]
**WV** velocity of wave propagation [m/s]
**TOF** time of flight [s]
**NDM** nondestructive method
**MCU** micro-controller unit
**IDE** integrated development environment
**UDP** user datagram protocol
**ADC** analog-digital converter
**DFT** discrete Fourier transform
**GPR** ground penetrating radar
**FWD** falling weight deflectometer
**RRRF** rail road response factor
**HT** Hilbert transform
**HV** hopper-vagon
**DTE** dynamic tamping express
**UVP-DIIT** a type of consolidation measurement device
**SV-20P** a type of geophone
**ESP32** a type of MCU
**ADS1256** a type of ADC

## References

[1] L. Fendrich, W. Fengler. *Handbuch Eisenbahninfrastruktur.* Second edition. Springer-Verlag Berlin Heidelberg, 2013. doi:10.1007/978-3-540-31707-4.

[2] S. Fischer. Breakage test of railway ballast materials with new laboratory method. *Periodica Polytechnica Civil Engineering* **61**(4):794–802, 2017. doi:10.3311/PPci.8549.

[3] L. Izvolt, J. Sestakova, M. Smalo. Tendencies in the development of operational quality of ballasted and ballastless track superstructure and transition areas. *IOP Conference Series: Materials Science and Engineering* **236**(1):012–038, 2017. doi:10.1088/1757-899X/236/1/012038.

[4] L. Izvolt, J. Harusinec, M. Smalo. Optimisation of transition areas between ballastless track and ballasted track in the area of the tunnel turecky vrch. *COMMUNICATIONS âĂŞ Scientific Letters of the University of Zilina* **20**(3):67–76, 2018.

[5] M. Sysyn, U. Gerber, V. Kovalchuk, O. Nabochenko. The complex phenomenological model for prediction of inhomogeneous deformations of railway ballast layer after tamping works. *Archives of Transport* **3**(46):91–107, 2018. doi:10.5604/01.3001.0012.6512.

[6] B. Wang, U. Martin, S. Rapp. Discrete element modeling of the single-particle crushing test for ballast stones. *Computers and Geotechnics* **88**:61–73, 2017. doi:10.1016/j.compgeo.2017.03.007.

[7] B. Lichtberger. *Handbuch Gleis: Unterbau, Oberbau, Instandhaltung, Wirtschaftlichkeit.* Second edition. Hamburg: Tetzlaff Verlag, 2003.

[8] S. Fischer, E. Juhász. Railroad ballast particle breakage with unique laboratory test method. *Acta Technica Jaurinensis* **12**(1):26–54, 2019. doi:10.14513/actatechjaur.v12.n1.489.

[9] L. Izvolt, J. Sestakova, M. Smalo. Analysis of results of monitoring and prediction of quality development of ballasted and ballastless track superstructure and its transition areas. *COMMUNICATIONS âĂŞ Scientific Letters of the University of Zilina* **18**(4):19–29, 2016.

[10] V. Kovalchuk, Y. Kovalchuk, M. Sysyn, et al. Estimation of carrying capacity of metallic corrugated structures of the type multiplate mp 150 during interaction with backfill soil. *EasternEuropean Journal of Enterprise Technologies* **1**(91):18–26, 2018. doi:10.15587/1729-4061.2018.123002.

[11] O. Nabochenko, M. Sysyn, V. Kovalchuk, et al. Studying the railroad track geometry deterioration as a result of an uneven subsidence of the ballast layer. *Eastern-European Journal of Enterprise Technologies* **97**(1):50–59, 2019. doi:10.15587/1729-4061.2019.154864.

[12] A. Atamanyuk. *The technology for ballast layer compaction with machines of type VPO after deep cleaning of ballast layer.* PhD Thesis:. Sankt-Petetrsburg State University of Railway Transport, 2010.

[13] R. D. Bold. *Non-Destructive Evaluation of Railway Trackbed Ballast.* PhD Thesis:. Institute for Infrastructure and Environment, School of Engineering, University of Edinburgh, 2011.

[14] J. Sadeghi, M. Motieyan-Najar, J. Zakeri, et al. Improvement of railway ballast maintenance approach, incorporating ballast geometry and fouling conditions. *Journal of Applied Geophysics* **151**:263–273, 2006. doi:10.1016/j.jappgeo.2018.02.020.

[15] R. D. Bold, G. OâĂŹConnor, J. Morrissey, M. Forde. Benchmarking large scale gpr experiments on railway ballast. *Construction and Building Materials* **92**:31–42, 2015. doi:10.1016/j.conbuildmat.2014.09.036.

[16] A. Glickman. About the principles of the spectral seismic survey. *Geology, geophysics and development of oil and gas fields* **12**:19–24, 1998.

[17] J. Sadeghi. Field investigation on dynamics of railway track pre-stressed concrete sleepers. *Advances in Structural Engineering* **13**(1):139–151, 2010. doi:10.1260/1369-4332.13.1.139.

[18] C. Esveld. *Modern railway track.* Second edition. MRT-Production, 2001.

[19] H. Lam, M. Wong. Railway ballast diagnose through impact hammer test. *Procedia Engineering The Twelfth East Asia-Pacific Conference on Structural Engineering and Construction* **14**:185–194, 2011. doi:10.1016/j.proeng.2011.07.022.

[20] J. Smutny, V. Nohal. Vibration analysis in the gravel ballast by measuring stone method. *Akustika* **25**(1):22–28, 2016.

[21] J. Sadeghi, P. Barati. Comparisons of the mechanical properties of timber, steel and concrete sleepers. *Structure and Infrastructure Engineering* **8**(12):1151–1159, 2012. doi:10.1080/15732479.2010.507706.

[22] M. Sysyn, V. Kovalchuk, D. Jiang. Performance study of the inertial monitoring method for railway turnouts. *International Journal of Rail Transportation* **4**(4), 2018. doi:10.1080/23248378.2018.1514282.

[23] J. Sadeghi. Effect of unsupported sleepers on rail track dynamic behavior. *Proceedings of the Institution of Civil Engineers âĂŞ Transport* **171**(5):286–298, 2018. DOI:doi:10.1680/jtran.16.00161.

[24] F. Ghofrani, Q. Hea, R. Goverdec, X. Liud. Recent applications of big data analytics in railway transportation systems: A survey. *Transportation Research Part C: Emerging Technologies* **90**:226–246, 2018. DOI:10.1016/j.trc.2018.03.010.

[25] A. Lasisi, N. Attoh-Okine. Principal components analysis and track quality index: A machine learning approach. *Transportation Research Part C: Emerging Technologies* **91**:230–248, 2018. DOI:10.1016/j.trc.2018.04.001.

[26] G. Lederman, S. Chen, J. Garrett, et al. A data fusion approach for track monitoring from multiple in-service trains. *Mechanical Systems and Signal Processing* **95**:363–379, 2017. DOI:10.1016/j.ymssp.2016.06.041.

[27] M. Sysyn, D. Gruen, U. Gerber, et al. Turnout monitoring with vehicle based inertial measurements of operational trains: a machine learning approach. *COMMUNICATIONS âĂŞ Scientific Letters of the University of Zilina* **21**(1):42–48, 2019.

[28] S. Rapp, U. Martin, M. StrÃďhle, M. Scheffbuch. Track-vehicle scale model for evaluating local track defects detection methods. *Transportation Geotechnics* **19**:9–18, 2019. DOI:10.1016/j.jrtpm.2016.03.001.

[29] M. Sysyn, U. Gerber, V. Rybkin, O. Nabochenko. Determination of the ballast layer degree compaction with dynamic and kinematic analysis of the acoustic waves impacts. *Sborník přednášek Železniční Dopravní Cesta VOŠ a SPŠ stavební* pp. 123–130, 2010.

[30] J. Mathews, K. Fink. *Numerical methods using Matlab.* Third edition. Williams Publishing House, 2001.

[31] A. Sergiyenko. *Digital signal processing.* Second edition. SPb: Piter, 2003.

[32] D. Larose, T. Larose. *Discovering knowledge in data: an introduction to data mining.* Second edition. Wiley, 2014.

[33] F. Heijden, R. Duin, D. Ridder, D. Tax. *Classification, Parameter Estimation and State Estimation: An Engineering Approach Using MATLAB.* Second edition. John Wiley & Sons, 2014.